

# OVERTOPPING FLOW IMPACT ON A VERTICAL WALL ON A DIKE CREST

Xuexue Chen<sup>1</sup>, Bas Hofland<sup>2</sup>, Corrado Altomare<sup>3,4</sup>, Wim Uijtewaal<sup>1</sup>

In this paper the impact process and mechanism of overtopping flow on a vertical wall on a dike crest are investigated by means of a series of physical model tests. A double-peaked force was recognized in a time series of an overtopping flow. Four stages were summarized for the whole overtopping flow impact process. An empirical relationship between the maximum impact pressure and impact rising time was found. By using the pressure impulse concept, the empirically established constant product of maximum impact pressure and rising time can be used to develop new design formula in the future.

*Keywords: Overtopping flow; Impact mechanism; Vertical wall; Dike*

## INTRODUCTION

In a populated coastal town of a low-lying country (e.g., the Netherlands, Belgium), a dike often has a wide crest which serves as an urbanized frontage. When the dike crest is lower than the water level or wave run-up height, overtopping occurs. The extreme overtopping event would bring considerable volumes of water with a certain velocity over the dike crest and towards inland. We label this fast moving water induced by overtopping as overtopping flow. Overtopping flow imposes a serious threat to both people and structures on the dike crest. Therefore, it is important for designers and owners to recognize the key hazards (e.g., building damage) from the overtopping flow.

Chen et al. (2012), De Rouck et al. (2012) and Ramachandran et al. (2012) reported their laboratory work of overtopping flow loads on vertical structures on a dike crest by physical models at different scales. Common findings of these works suggested that the observed force evolution shape of overtopping flow has a double-peak, which is similar to the “church-roof” time history of wave breaking impact force proposed by Oumeraci et al. (1993) for deeper water wave impacts on caissons and composite structures. However, the overtopping flow is a bore-like transition wave. The classification of wave impact mechanism, which is based on the location of wave breaking (Oumeraci et al., 1993), is not suitable for this study. Therefore, the impact mechanisms of overtopping flow and the unique flow characteristics need to be understood.

The aim of this paper is to understand the impact process of overtopping flow by measuring the flow field in front of the wall and its resultant impact pressure on a vertical wall.

## EXPERIMENT SET-UP

### Facilities and wall model

Physical model tests were performed in a 4 m wide, 1.4 m deep and 70 m long wave flume at Flanders Hydraulic Research, Antwerp, Belgium. A piston-type wave generator with a stroke length of 0.6 m was used to generate monochromatic, multi-chromatic and random waves, but without an active wave absorption system. The wave flume was split into four sections (1 m for each), as shown in Figure 1. A wall model consisting of two parts: a force-measuring portion and a fixed wall. Two load cells of model series Tedeo-Huntleigh 614 were used to determine the total overtopping flow force with sampling rate of 1000 Hz, which were mounted with the aluminum plate. Next to the force-measuring portion, four point pressure sensors were mounted on the face of the wall, see Figure 2. They are sampled at a rate of 1000 Hz in order to detail the local pressure evolution and to help understand the impact mechanism of the overtopping flow. The lowest sensor ( $P_1$ ) was mounted 3.5 cm above the dike crest and the space between the two centers of each sensor was 4 cm. Details about the facilities and wall model can be referred to Chen et al. (2014).

### Bubble Image Veocimetry

Due to a series of wave breaking processes on the foreshore, the generated overtopping flow on the dike is a highly aerated flow. This complex flow characteristics limits accurate measurement of the overtopping flow features (De Rouck et al., 2012). In this study, Bubble Image Velocimetry (BIV) technique developed by Ryu et al. (2005) was applied to measure the flow velocity field in front of the wall. This technique has been proven sufficiently to measure this kind of flow (e.g., Ryu et al., 2007; Pedrozo-Acuña et al., 2011;

<sup>1</sup>Dept. of Hydraulic Eng., Delft University of Technology, Stevinweg 1, 2628 CN Delft, The Netherlands

<sup>2</sup>Dept. of Coastal Structures and Waves, Deltares, PO Box 177, 2600 MH Delft, The Netherlands

<sup>3</sup>Flanders Hydraulics Research, Berchemlei 115, 2140 Antwerp, Belgium

<sup>4</sup>Ghent University, Technologiepark 904, B-9052 Ghent, Belgium

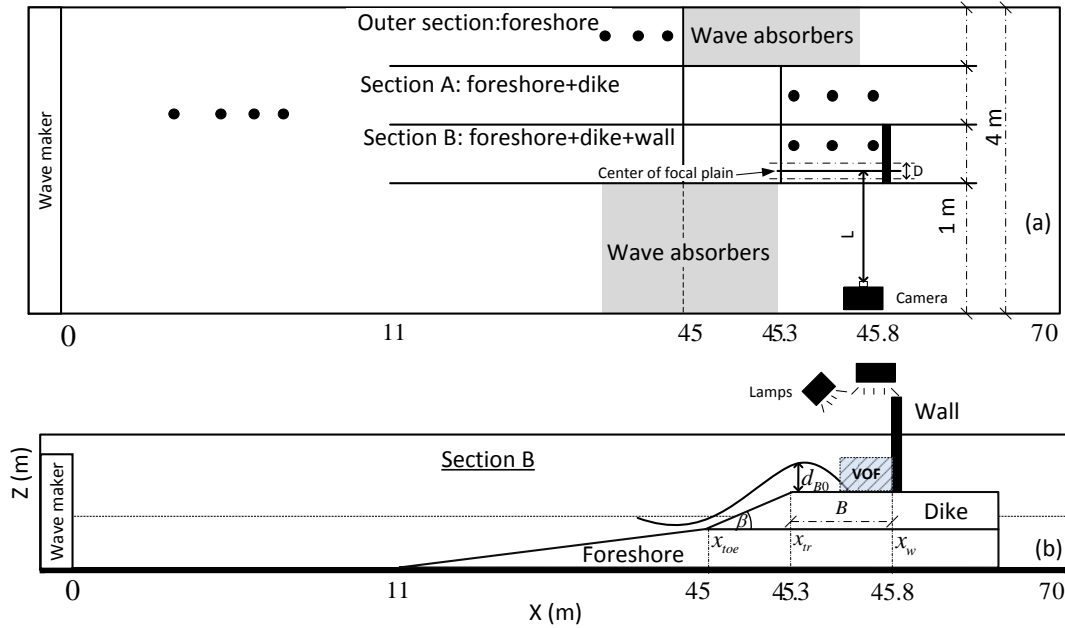


Figure 1: Wave flume in Flanders Hydraulic Research (Antwerp, Belgium). (a) is a top view of the flume, (b) is the respective section B to measure impact forces and velocity field.

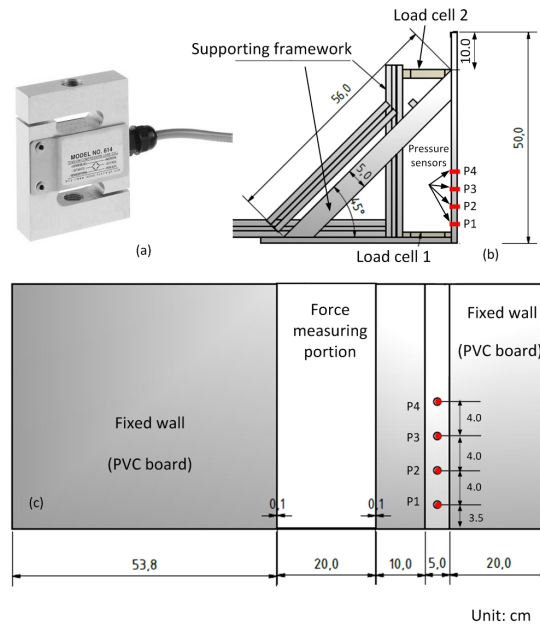


Figure 2: Wall model and force measuring system including (a) load cell (b) positioning of load cells and supported frameworks and (c) front view of wall model and locations of pressure sensors

Lin et al., 2012; Ariyaratne et al., 2012; Song et al., 2013). The BIV set-up of this study with top lighting provided by two Fresnel lights (500 W and 1000 W) were placed above the domain of interest, as shown in Figure 1b. A high speed camera (SpeedCam MiniVis e2) with a  $512 \times 512$  CMOS sensor recored images with a field of view (FOV) of  $0.23 \times 0.18 \text{ m}^2$  that covered the main part of overtopping flow in front of the wall model, as shown in Figure 1b. The center of focal plane is 0.05 m behind the glass wall, the depth of

field (DOF) is 0.055-0.08 m, which is calculated by using focal distance  $L = 0.95m$ , value for the circle of confusion  $c = 0.008m$ ,  $f = 25$  mm and  $N = 2 - 2.8$ . Details of the calculation formula and definition of each parameter can be found from Ryu et al. (2005).

The camera was sampling at 1000 frames per second throughout the impact processes of the second and the third overtopping flows of one experiment. The flow surface in each image was detected, color inverted and then cross-correlated to obtain the instantaneous velocities using PIV software from PIVlab developed by William Thielicke. The velocity determination was with a  $32 \times 32$  pixel interrogation area with a 50% overlap between adjacent interrogation areas.

### Test program and data processing

The testing program of this paper was restricted to series of regular waves repeated 36 times with a condition of  $h_0 = 1$  m,  $H_0 = 0.2$  m,  $T_0 = 4$  s,  $B = 0.5$  m and  $\cot\beta = 3$ , where  $h_0$  is offshore water depth,  $T_0$  is offshore wave period,  $H_0$  is offshore wave height,  $B$  is the distance of wall to the seaward side of dike crest,  $\cot\beta$  is dike seaward slope. Good test repeatability resulted in an averaged 0.24% standard deviation of overtopping flow depth  $d_{B0}$ . The forces and impact pressures from the second and the third overtopping impact events of each test, which were considered representative, were analyzed. The raw signal of pressure sensors was not filtered because of the low noise level of pressure sensors.

## RESULTS

### General observation

Impact pressure from each event is different because of the air entrainment within the turbulent overtopping flow. Even though the tests were conducted with regular waves, the individual impact force of subsequent incoming waves still shows irregular magnitude and different double-peak shapes. Figure 3 provides an example of impact force signals from the second and third overtopping events. The red line indicates the total horizontal force measured by load cells and the other four lines ( $P1$  to  $P4$ ) illustrate the time series of pressure sensors. The force and pressure measuring system are depicted in to Figure 2. From time histories of  $P_1$ , we can recognize the initial impact peak with short duration and a quasi-static peak with long duration. It is interesting to see that the ratios of impact duration ( $\bar{t}_d$ ) and wave period at the dike toe  $T$  are 0.0075 and 0.01 respectively, which are in order of impact loading with  $\bar{t}_d/T \approx 0.001 \sim 0.01$  (Oumeraci et al., 2001). However the ratios of initial impact force peak ( $F_{im}$ ) and quasi-static impact peak ( $F_{eq}$ ) are about 1 and 1.5 which is outside the range of impact loading defined by Kortenhaus and Oumeraci (1998) as  $F_{im}/F_{eq} > 2.5$ . Thus, the overtopping flow initial impact force is not a real impact at least within this study.

Based on the observations, the overtopping flow could be influenced by the previous overtopping event. There are two basic situations that can describe this influence, defined as "interaction" and "wet bed". For the interaction situation, it means the collision between the subsequent incoming wave and the previous reflected wave on the dike, whereas the "wet bed" situation means the previous wave only leaves a residual water layer on the dike before the subsequent overtopping flow generates. In the regular wave condition, only the "wet bed" situation was considered (see Figure 4).

### Impact processes

The overtopping impact processes of the second and third overtopping events of each tests were captured by the high speed camera with a sampling rate of 1000 fps. An example of the second overtopping event of test No. Sine-028-26 is shown in Figure 5. Based on the different dominant physical mechanisms, a whole impingement process can be divided into four stages: pre-impact, Figure 5 (a)-(c); initial impact, Figure 5 (d)-(e); continued deflection, Figure 5 (f)-(i), and reflection in Figure 5 (j)-(l). The instant pressure distributions of the same snapshot moments and time series of four pressure sensors are shown in Figure 6 and Figure 3a. From Figure 3a, two distinct peaks can be seen from pressure signals of  $P1$  (black line), whereas a tiny peak is shown before the initial impact peak and a terrace shape pressure evolution after the quasi-static impact peak can also be recognized. Due to lacking the pressure information just at bottom of the wall, it is expected that the tiny peak and the initial impact peak would be larger. Details of each stage are described below:

- Pre-impact stage

After passing the dike crest transition line ( $x_{tr}$ ), the overtopping flow is approaching the wall with a wedge shape from left to right, see Figure 5 (a). An irregular tiny tip, moving over the residual water present on

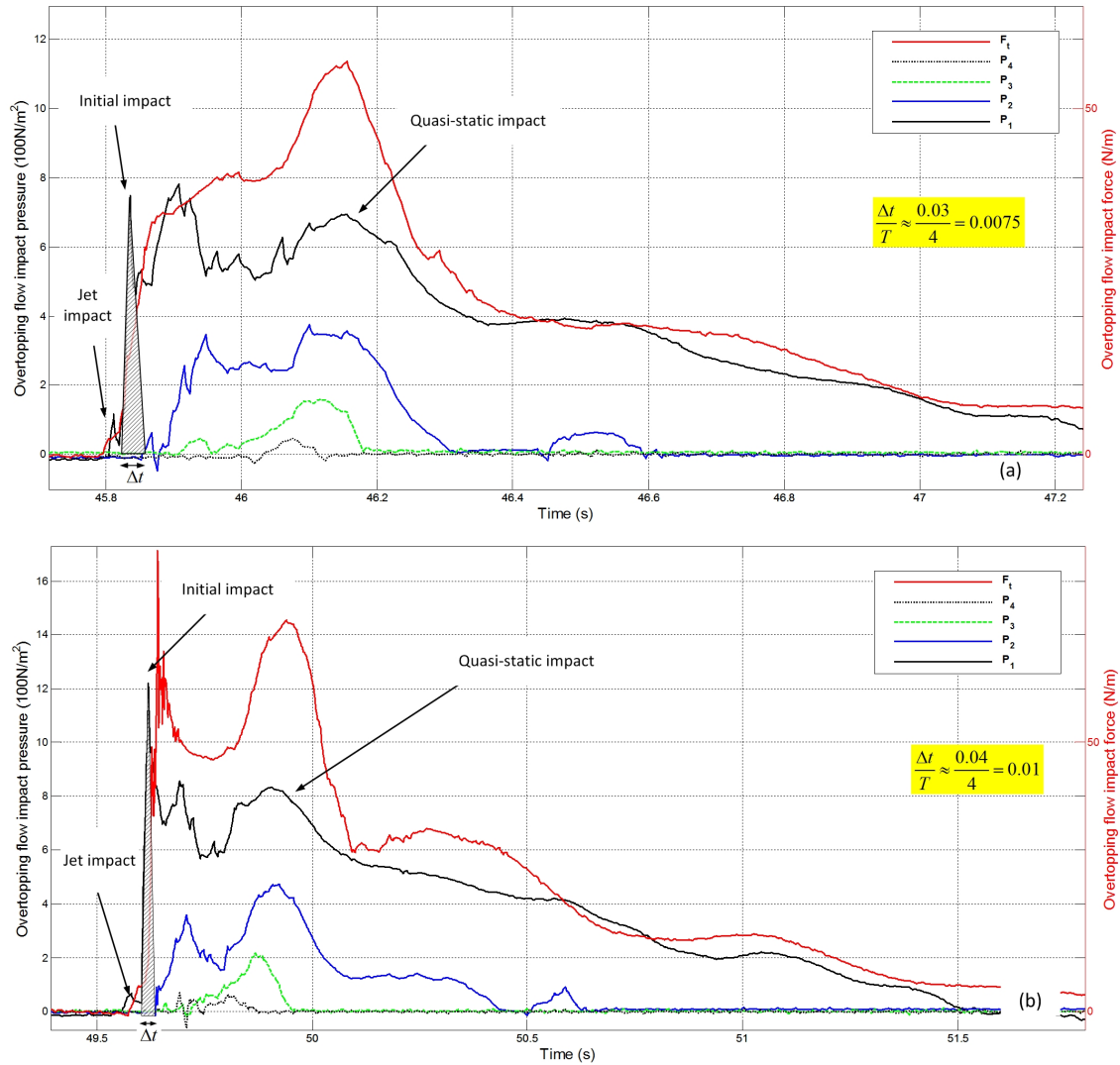


Figure 3: Example of the time series signals of total force from load cell and pressure sensors. (a) is from the second overtopping event shown in Figure and (b) is from the third event shown in Figure.  $\Delta t$  is the approximate impact duration and  $T$  is the incoming wave period

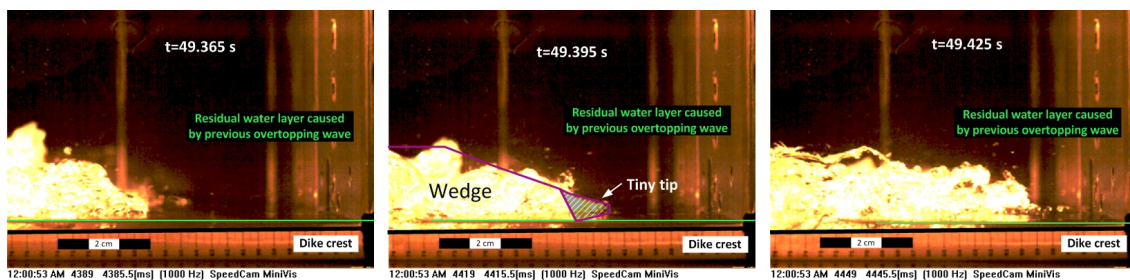
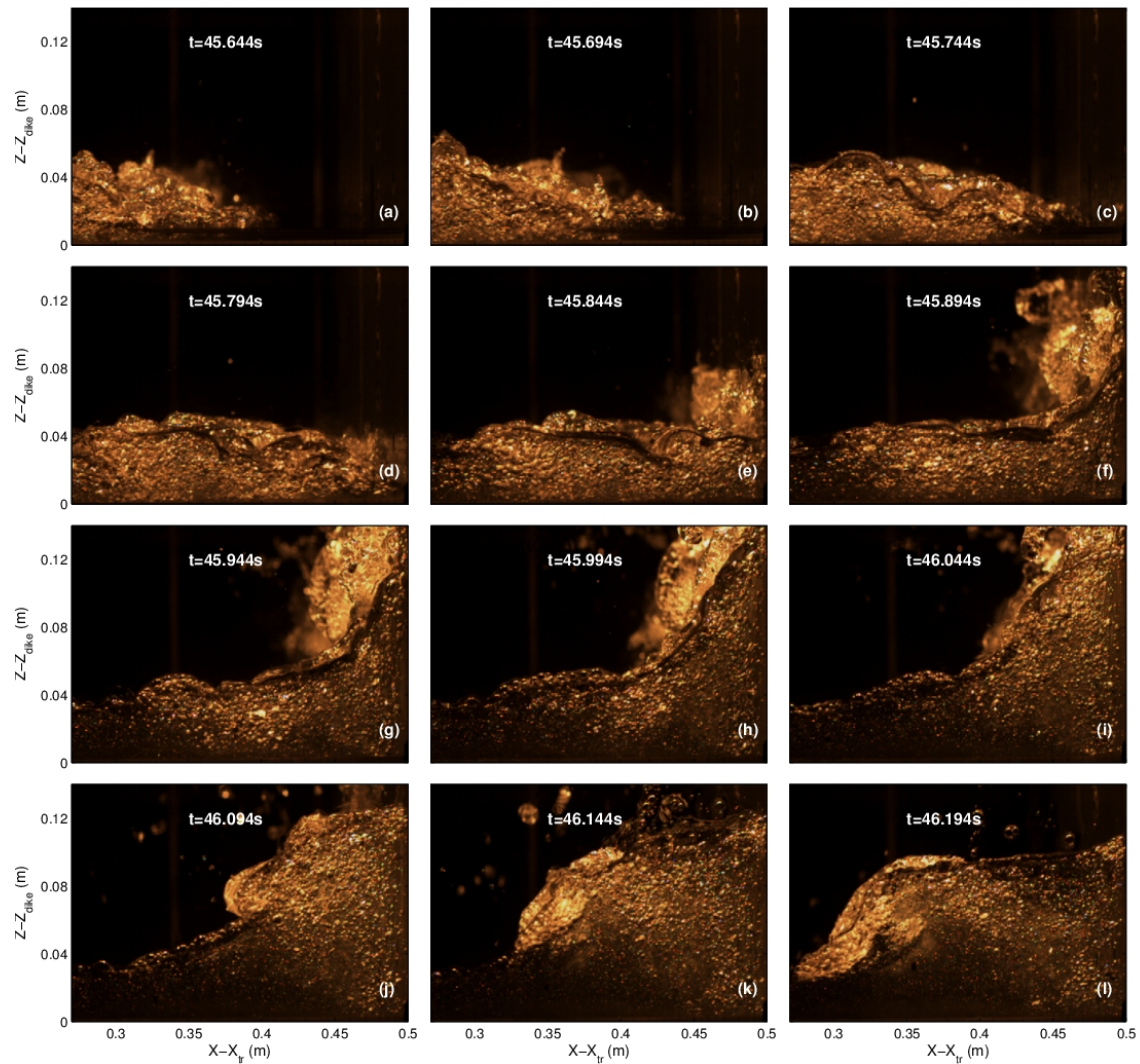


Figure 4: Snapshot of the third overtopping event of test No.Sine-028-26:  $H_0 = 0.2$  m,  $T_0 = 4$  s,  $h_0 = 1$  m,  $B = 0.5$  m and  $\cot\beta = 3$ . The green line indicates the residual water level on dike crest. Note that the raw images have been adjusted by increasing the exposure value from 0 to 6.



**Figure 5: An example of the overtopping flow impact process of the second wave of test No.Sine-028-26. Note that  $x - x_{tr}$  and  $z - z_{dike}$  are the horizontal and vertical coordinate of dike crest. The wall is located at  $x - x_{tr} = 0.5$  m**

the crest (Figure 4), is ahead of the wedge (Figure 5 (b)-(c)). The turbulent fluctuations in the flow front are expected to generate local pressure fluctuations.

- Initial impact stage:

Figure 5 (d)-(e) show the initial impulse process, which can be divided into two subprocesses: tiny jet impact and initial main impact.

When the flow tip touches the wall face, a rapid rising tip forms a vertical jet earlier than the initial impact of the wedge. From Figure 3, we can observe this initial jet impact from time history of  $P1$ . The tiny peak before the main initial impact peak indicates this jet impact. It is assumed that the vertical jet dampens the main impact during the initial impact stage. Oumeraci et al. (1993) gave a similar description for a bore impact process. They stated that a bore consists of two parts, including a steep turbulent front and a rear of the water mass. The foamy front part strikes the wall first and then is squeezed by the following impacting "pure" water. This "pure" water impact is significantly dampened by the earlier foamy mass which is then deflected upwards. Whereas in the overtopping flow situation, the jet is the result of direct impact of a turbulent tip on the wall. Peregrine (2003) defined a 'flip-through' term to describe a rising jet

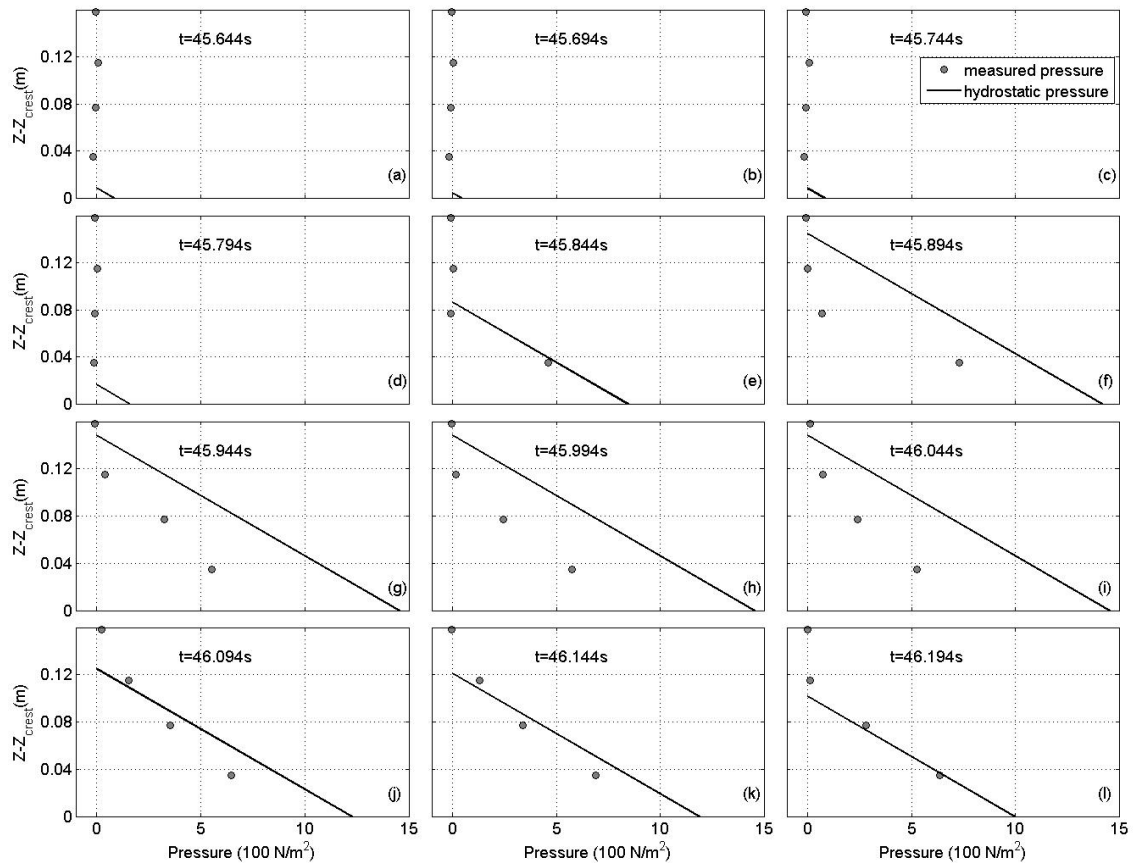


**Figure 6: Instant measured pressure (gray marker) and computed hydrostatic pressure ( $= \rho gh_{max}$ ) (solid line),  $h_{max}$  is the highest water surface elevation at  $x_w$  extracted from raw image.**

filling the gap between wall and wave during a wave impact process in deep water condition. This is similar to the filling process of overtopping flow tip but the generation mechanism is different. In Peregrine's potential flow computational work, the rising jet forms from the volume flux beneath the incoming wave crest (Bredmose et al., 2009). Due to  $P_1$  was mounted at 3.5 cm above dike crest, the largest pressure of the tiny jet impact information was not observed, thus the jet cushion will be investigated in future work.

When the wedge touches the wall, the flow front changes its direction suddenly (Figure 5 (e)-(f)) and results in a sharp dynamic impact pressure at  $P_1$  (Figure 6 (e)-(f)). This is the 1<sup>st</sup> main peak shown in Figure 3 named as initial impact. During this process, the kinetic energy is changing into potential energy. The short duration of the initial impact pressure could only influence local structural elements with a high natural frequency.

- Deflection stage :

After initial impact, the following wedge continues rising up the face of the wall until it reaches the maximum run-up height. During this stage, the kinetic energy is converted into potential energy totally. Figure 5 (g)-(i) show snapshots of run-up and down-rush of the deflected water. The corresponding instant pressure distribution along the wall is shown in Figures 6 (g)-(i), in which the solid line indicates the computed hydrostatic pressure distribution using the detected run-up surface elevation from high speed image and the markers indicate that of measured instant pressure. The linear distribution of instant pressure shows a quasi-static nature of impact pressure in this stage which is smaller than computed hydrostatic pressure.

- Reflection stage:

When the deflected water approaching to the maximum run-up level, it starts falling onto the remaining un-splashed part of the incident flow and is advancing seawards (Figure 5 (i)-(l)). The second peak shown in

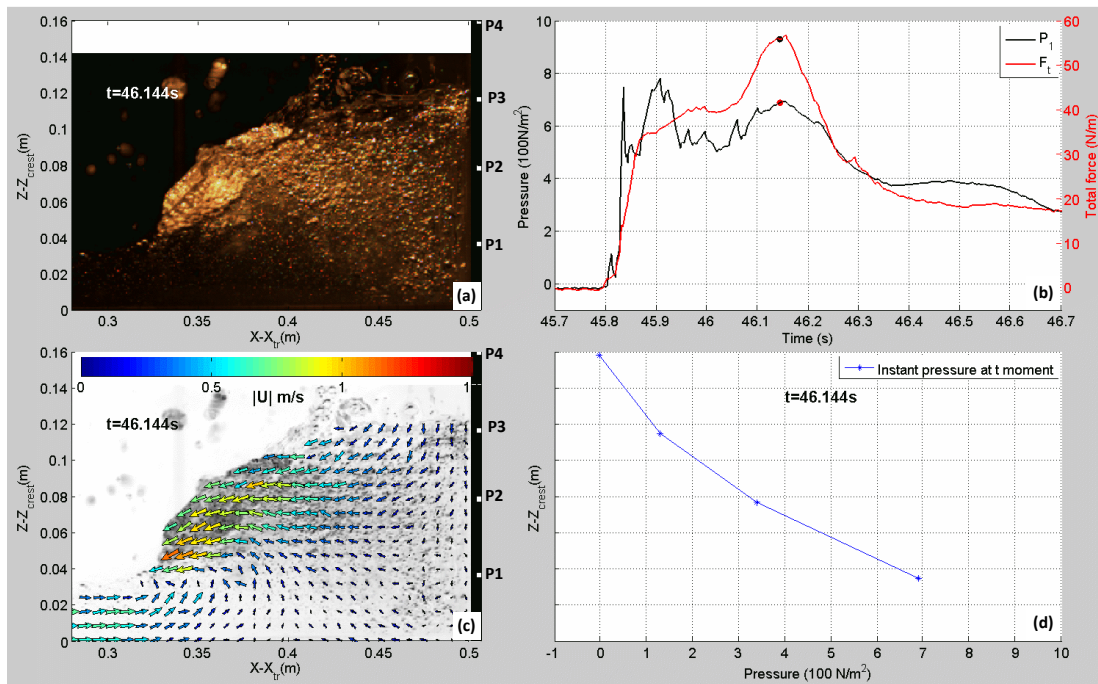


**Figure 7: An example of measured flow field at the moment of the 2nd impact force peak occurrences. (a) raw high speed image at  $t=46.144$  s; (b) impact time series of P1 (black) and total force obtained from load cell (red); (c) velocity field at the  $t=46.144$  s; and (d) instant measure pressure distribution at the same moment.**

Figure 3 is generated during this stage (Figure 6 (j)-(k)). Figure 7 shows a group of flow features (raw high speed image, velocity field and instant pressure distribution) at the moment of  $t=46.144$  s. The zero velocity vectors close to the wall in Figure 7 (c) and almost linearly distributed instant pressures in Figure 7 (d) indicate the quasi-static nature of 2nd force peak shown in Figure 7 (b). This quasi-hydrostatic pressure is governed by gravity. Figure 5 (i)-(l) specify the formation of reflected bore. The terrace shape signal behind the 2nd peak means the reflected bore is undulated. When the reflected bore is fully developed, the instant pressure is same as that of computed for the hydrostatic pressure, see Figure 6 (l)

#### Impact maximum pressure and rising time $t_r$

Based on the concept of constant impulse during the wave impact, a relation between maximum impact pressure  $P_{im}$  and impact rising time  $t_r$  can be built (e.g., Weggel and Maxwell; Salih Kirkgöz, 1990; Hattori et al., 1994; Cuomo et al., 2011; Ariyaratne et al., 2012). The definition of  $t_r$  can be referred to Fig.2 from Cuomo et al. (2011). Most of the researchers have been reported that there is a relationship between  $P_{im}$  and  $t_r$ :

$$P_{im} = at_r^b, \quad (1)$$

where  $a$  and  $b$  are empirical dimensional coefficients.  $b$  is within a range of -0.6 to -1, owing to different experimental configurations (Ariyaratne et al., 2012). Also the level of aeration would affect the rising time (e.g., Blackmore and Hewson, 1984; Bullock et al., 2001). Within these studies, the wave impact of Ariyaratne et al. (2012) is induced by overtopping flow (green water in their work), which is similar to the current situation.

Following Eq. (1), measured  $P_{im}$  and  $t_r$  were plotted in Figure 8. The solid line is the best fit curve, and the dashed line is the envelope curve for the test data. A similar conclusion was also obtained by other researchers. The value of  $b = -0.79$ ,  $a=41$  and  $a=130$  for the envelope curve obtained from the present results agrees well with that of Ariyaratne et al. (2012).

By using the constant impulse concept (Peregrine, 2003),  $b$  value was forced to -1 subjectively. Then

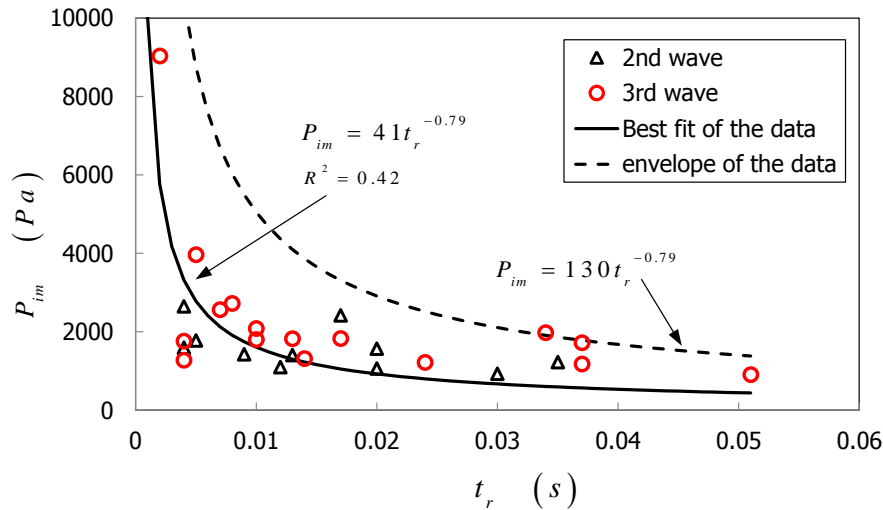


Figure 8: A relation of impact maximum pressure  $P_{im}$  and rising time  $t_r$  of  $P_1$ , triangle marker illustrates the data from the 2nd overtopping flow, whereas circles are the 3rd wave impact of each test.

Eq.(1) can be rewritten as:

$$P_{im} t_r = c, \quad (2)$$

where  $c=13.43$  is constant value, determined empirically by curve fitting, see Figure 9.

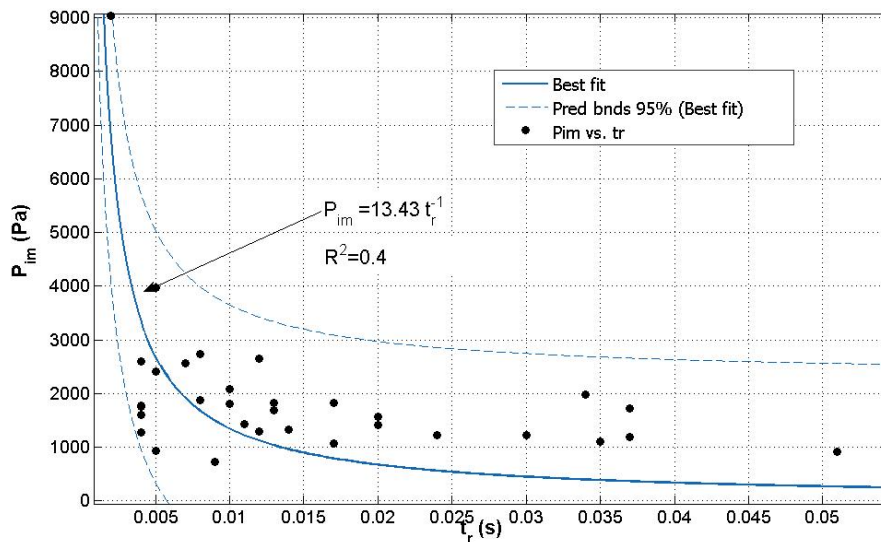


Figure 9: Re-plotting impact maximum pressure  $P_{im}$  and rising time  $t_r$  of  $P_1$  by forcing  $b=-1$ . Data points are from the 2nd and 3rd waves, as shown in Figure 8. Solid line is the best fit curve, and dashed lines are the 95% confidence interval.

## CONCLUSION

In this study, the impact process and mechanism of overtopping flow on dike crest were presented based on regular wave tests. The findings can be summarized as:

- 1) Four stages of impact and a double peaked force signal:

The whole impact process can be divided into four stages: pre-impact, initial impact, deflection, and

reflection. The maximum total force occurs at later phase of deflection or early phase of reflection. The time series of overtopping flow load shows a double-peak shape. This shape is in line with the existing knowledge of wave impact force, though the magnitude differs from the real “impact” defined by Oumeraci et al. (2001). There are some observations different from existing literature. One difference is the initial impact format which is similar to a slightly breaking wave impact. The other one is the occurrence of the jet impact (a tiny peak shown in the time series of force), which is believed causing by the impingement of the turbulent flow front. Due to lacking the information of pressure at the locations below  $P_1$ , the influence of jet impact on the initial impact need to be investigated in the future.

2) Effects of previous flow events

The wide crest of the dike and the appearance of the wall contribute a unique interaction pattern between the previous flow and the successive flow on the dike. In the current regular wave test, the previous flow had gone back to the flume before the successive flow generated on the dike. So only the residual water layer left by the previous flow will influence the following flow. In the future, other interaction patterns will be investigated.

3) Velocity field of overtopping flow

The BIV technique was used to measure the flow velocity field during the impact process. In this paper, only some preliminary results were presented, from which the velocity field at the moment of 2nd impact peak occurrence was observed and which provided a proof of the quasi-hydrostatic nature of this peak. In the future study, the relationship between the flow velocity field at pre-impact stage and initial impact peak need to be investigated because of the importance of initial impact to design a stiff structure.

4) Maximum impact pressure prediction

A empirical relation between maximum impact pressure  $P_{im}$  and rising time  $t_r$  was built, which is in line with that from other studies. The modified relationship of  $P_{im}$  and  $t_r$  by using impulse concept (Eq.(2)) results in a constant product ( $c=13.43$  in this study). This constant product can be used to calculate the design impact pressure by changing the predicted rising time  $t_r$  for different structures which suffer from same impact load or the other way around. However, in this study, only one wave condition was tested. In the future, a wider parameter range need to be tested, and the resultant constant product of each condition need to be expressed empirically by using incident wave and dike geometry characteristics.

#### ACKNOWLEDGEMENTS

We gratefully acknowledge the technical staff of Flanders Hydraulics Research and hydraulic laboratory of Delft University of Technology for their great assistance to conduct the experiments. The present work is sponsored by STW-programme on integral and sustainable design of multifunctional flood defences, Project No.12760, Flanders Hydraulic Research, and the WTI 2017 project (“Research and development of safety assessment tools of Dutch flood defences”), commissioned by the department WVL of Rijkswaterstaat in the Netherlands.

#### References

- Ariyaratne, K., Chang, K.-A., and Mercier, R. 2012. Green water impact pressure on a three-dimensional model structure. *Experiments in Fluids*, 53(6):1879–1894
- Blackmore, P. and Hewson, P. 1984. Experiments on full-scale wave impact pressures. *Coastal Engineering*, 8(4):331–346
- Bredmose, H., Peregrine, D. H., and Bullock, G. N. 2009. Violent breaking wave impacts. Part 2: modelling the effect of air. *Journal of Fluid Mechanics*, 641:389
- Bullock, G., Crawford, A., Hewson, P., Walkden, M., and Bird, P. 2001. The influence of air and scale on wave impact pressures. *Coastal Engineering*, 42(4):291–312.

- Chen, X., Hassan, W., Uijtewaal, W., Verwaest, T., Verhagen, H. J., Suzuki, T., and Jonkman, S. N. 2012. HYDRODYNAMIC LOAD ON THE BUILDING CAUSED BY OVERTOPPING WAVES. *Coastal Engineering Proceedings*, 1(33):structures.59
- Chen, X., Hofland, B., Altomare, C., Suzuki, T., and Uijtewaal, W. 2014. Forces on a vertical wall on a dike crest due to overtopping flow. *Coastal Engineering* (Accepted)
- Cuomo, G., Piscopia, R., and Allsop, W. 2011. Evaluation of wave impact loads on caisson breakwaters based on joint probability of impact maxima and rise times. *Coastal Engineering*, 58(1):9–27
- De Rouck, J., Van Doorslaer, K., Versluys, T., Ramachandran, K., Schimmels, S., Kudella, M., and Trouw, K. 2012. FULL SCALE IMPACT TESTS OF AN OVERTOPPING BORE ON A VERTICAL WALL IN THE LARGE WAVE FLUME (GWK) IN HANNOVER. *Coastal Engineering Proceedings*, 1(33):structures.62.
- Hattori, M., Arami, A., and Yui, T. 1994. Wave impact pressure on vertical walls under breaking waves of various types. *Coastal Engineering*, 22(1-2):79–114.
- Kortenhaus, A. and Oumeraci, H. 1998. CLASSIFICATION OF WAVE LOADING ON MONOLITHIC COASTAL STRUCTURES
- Lin, C., Hsieh, S.-C., Lin, I.-J., Chang, K.-A., and Raikar, R. V. 2012. Flow property and self-similarity in steady hydraulic jumps. *Experiments in Fluids*, 53(5):1591–1616.
- Oumeraci, H., Klammer, P., and Partenscky, H. 1993. Classification of breaking wave loads on vertical structures. *Journal of Waterway, Port, Coastal, and Ocean Engineering*, 119(4):381–397.
- Oumeraci, H., Kortenhaus, A., Allsop, W., de Groot, M., Crouch, R., Vrijling, H., and Voortman, H. 2001. *Probabilistic Design Tools for Vertical Breakwaters*.
- Pedrozo-Acuña, A., de Alegría-Arzaburu, A. R., Torres-Freyermuth, A., Mendoza, E., and Silva, R. 2011. Laboratory investigation of pressure gradients induced by plunging breakers. *Coastal Engineering*, 58(8):722–738,
- Peregrine, D. H. 2003. Water-wave impact on walls. *Annual Review of Fluid Mechanics*, 35(1):23–43.
- Ramachandran, K., Genzalez, R. R., Oumeraci, H., Schimmels, S., Kudella, M., Van Doorslaer, K., De Rouck, J., Versluys, T., and Trouw, K. 2012. LOADING OF VERTICAL WALLS BY OVERTOPPING BORES USING PRESSURE AND FORCE SENSORS - A LARGE SCALE MODEL STUDY. *Coastal Engineering Proceedings*, 1(33):currents.44.
- Ryu, Y., Chang, K.-A., and Lim, H.-J. 2005. Use of bubble image velocimetry for measurement of plunging wave impinging on structure and associated greenwater. *Measurement Science and Technology*, 16(10):1945–1953.
- Ryu, Y., Chang, K.-A., and Mercier, R. 2007. Application of dam-break flow to green water prediction. *Applied Ocean Research*, 29(3):128–136.
- Salih Kirkgöz, M. 1990. An experimental investigation of a vertical wall response to breaking wave impact. *Ocean Engineering*, 17(4):379–391.
- Song, Y. K., Chang, K.-A., Ryu, Y., and Kwon, S. H. 2013. Experimental study on flow kinematics and impact pressure in liquid sloshing. *Experiments in Fluids*, 54(9):1592.
- Weggel, J. R. and Maxwell, W. H. C. 1970. Numerical Model for Wave Pressure Distributions. *Journal of the Waterways, Harbors and Coastal Engineering Division*, 96(3):623–642.